IEEE Access
Multidisciplinary | Rapid Review | Open Access Journal

Received July 7, 2018, accepted August 21, 2018, date of publication August 29, 2018, date of current version September 28, 2018.

Digital Object Identifier 10.1109/ACCESS.2018.2867686

A Fast and Efficient Analytical Modeling Approach for External Electromagnetic Field Coupling to Transmission Lines in a Metallic Enclosure

LIPING YAN[1], (Senior Member, IEEE), XINDAN ZHANG[1], XIANG ZHAO[1], XIAOLAN ZHOU[1], AND RICHARD XIAN-KE GAO[2], (Senior Member, IEEE)

[1]College of Electronics and Information Engineering, Sichuan University, Chengdu 610065, China
[2]Institute of High Performance Computing, A*STAR, Singapore 138632

Corresponding author: Liping Yan (liping_yan@scu.edu.cn)

This work was supported by the National Natural Science Foundation of China under Grant NSAF-U1530143.

ABSTRACT A fast and efficient analytical approach based on the extended Baum-Liu-Tesche (BLT) equation is proposed in this paper to evaluate the external electromagnetic field coupling to transmission lines (TLs) loaded in a metallic enclosure with apertures. The scattering matrix to describe the aperture coupling characteristics required in the BLT equation is effectively derived based on the equivalent circuit theory. The analytical modeling function for calculating internal modal fields coupling to TLs is investigated and developed. Thus, the extended BLT equation can be directly employed in the assessment of current induced at the loads of TLs in the enclosure, which is illuminated by external electromagnetic fields. Via different case studies, the results calculated using the proposed analytical approach have been validated and have been in a good agreement with those simulated by numerical methods. The computational efficiency, in terms of time and memory, has also been improved much for the electromagnetic interference problems.

INDEX TERMS Aperture coupling, extended BLT equation, electromagnetic topology, field coupling to transmission lines.

I. INTRODUCTION

With the advancement of electronics and wireless technologies, the coupling between external electromagnetic (EM) field and transmission lines (TLs) in a metallic enclosure with apertures becomes more critical than before [1]–[3]. On one hand, there are more electromagnetic noises due to the introduction of more wireless devices and electronic systems. On the other hand, the apertures on the metallic shielding surfaces for necessary electrical connections and ventilation provide coupling paths between external EM fields and internal TLs. To evaluate the induced current at the loads of TLs for electromagnetic noise mitigation, a number of endeavors have been made either using numerical methods or analytical approaches. The numerical methods can address complicated configurations and offer precise results, yet are often time consuming and computationally intensive [1], [4]–[6]. Conventional analytical methods provide faster calculation and require much less computer resources but are only applicable for simple structures [7]–[10]. Several analytical methods have been proposed to investigate the internal EM field coupling to TLs in an enclosure, and the dyadic Green's function is applied to calculate the electric field [8], [9]. Some other analytical models have been developed to determine external EM field coupling to TLs within a cavity through apertures, where two circuit models are built to compute the electric field distribution in the enclosure [10]. However, these methods are not efficient for complicated configurations.

Electromagnetic topology (EMT) is an effective methodology to analyze EM pulse coupling to complicated electrical systems such as aircraft and satellites [11], [12]. Based on EMT, Tesche and Butler proposed an extended Baum-Liu-Tesche (BLT) equation for analyzing the EM field coupling to TLs [13]. The equation allows the TLs and apertures to be modeled together once the coupling functions and scattering matrix at the specified nodes are obtained.

However, the scattering characteristics of the aperture coupling or the electric field around the TLs had to be obtained by using numerical methods or from measurement [12], [14]. The coupling functions for field interaction with TLs are only applicable in a free space. Both limit the application of the extended BLT equation.

To overcome these weaknesses, the new and effective analytical functions for modal EM fields coupling to TLs in an enclosure (or limited space) and scattering function for

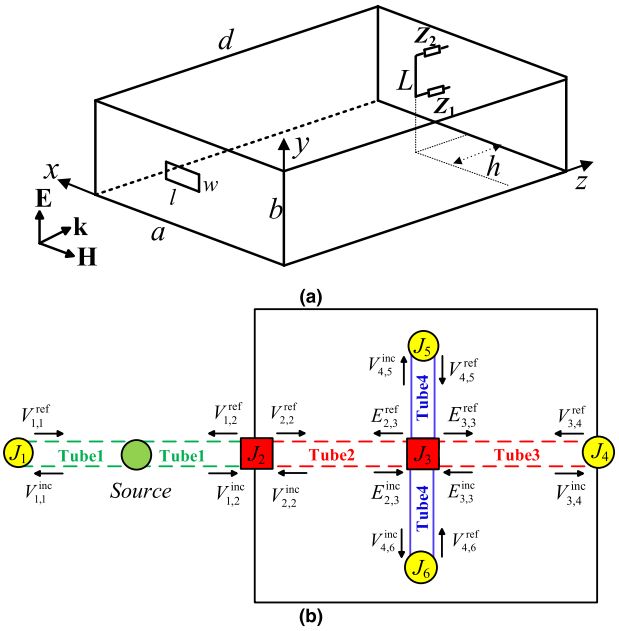

FIGURE 1. Calculation model: (a) geometrical model, and (b) signal flow diagram for the EM interaction geometry of (a).

aperture coupling are proposed in this study. Consequently, the extended BLT equation could directly examine the external EM field coupling to TLs in a metallic enclosure without any aid of numerical simulation or measurement. The calculated results agree well with those from the numerical simulation using the commercial tool CST [15]. Meanwhile, much less computational time and memory are consumed by using the proposed analytical method.

II. BLT-BASED ANALYTICAL MODELING

Consider a perfectly conductive rectangular enclosure containing one or multiple apertures on the front wall illuminated by an external electromagnetic field. A lossless transmission line of length L, which is parallel to the y-axis, is located at a distance h away from the back wall. The TL is terminated with the loads Z_1 and Z_2 located at (a/2, y_1, d) and (a/2, y_2, d), respectively, as shown in Fig. 1(a). The signal flow diagram [12] for the EM interaction geometry and the incident/reflected voltages or E-fields are illustrated in Fig. 1(b). Nodes J_1 and J_4 represent the observing point and the shorted end of the enclosure, respectively. Nodes J_5 and J_6 are the terminated loads of the TLs. Note that, the load is the general name of various components or elements that are connected to each end of the TL. These four nodes are the conventional nodes, which contain incident and reflected voltages and currents (or E and H-fields). Nodes J_2 and J_3 are another type of node denoted by square boxes, which contain EM field coupling and scattering information. Node J_2 stands for the aperture coupling, while node J_3 represents the modal fields coupling to the TLs.

There are also three tubes in the signal flow diagram (Fig. 1b). Tube 1 represents the field propagation in free space, while tube 2 and tube 3 depict the field propagation in the enclosure. All these propagation tubes are represented by dashed lines. Tube 4 is a TL tube and is denoted by the solid line. Note that the traveling wave component on each tube i at each node j is denoted by $V_{i,j}$ or $E_{i,j}$.

To apply the extended BLT equation to the whole field coupling analysis (from external to internal), both the node reflection relationship and the tube propagation relationship need to be examined. In particular, the scattering matrix at node J_2 and the coupling functions at the node J_3 should be determined first.

A. NODE REFLECTION RELATIONSHIP

Considering the reflection characteristics at nodes J_1, J_4, J_5 and J_6 and the scattering characteristics at nodes J_2 and J_3, the node reflection relationship is given as

$$[V]^{\text{ref}}_{8\times1} = [\rho]_{8\times8}[V]^{\text{inc}}_{8\times1} \tag{1}$$

where the reflection matrix is

$$[\rho] = \begin{bmatrix} \rho_1 & O_{1\times2} & O_{1\times2} & O_{1\times1} & O_{1\times1} & O_{1\times1} \\ O_{2\times1} & [\rho]_2 & O_{2\times2} & O_{2\times1} & O_{2\times1} & O_{2\times1} \\ O_{2\times1} & O_{2\times2} & [\rho]_3 & O_{2\times1} & O_{2\times1} & O_{2\times1} \\ O_{1\times1} & O_{1\times2} & O_{1\times2} & \rho_4 & O_{1\times1} & O_{1\times1} \\ O_{1\times1} & O_{1\times2} & O_{1\times2} & O_{1\times1} & \rho_5 & O_{1\times1} \\ O_{1\times1} & O_{1\times2} & O_{1\times2} & O_{1\times1} & O_{1\times1} & \rho_6 \end{bmatrix} \tag{2}$$

and the incident and reflected voltages are

$$[V]^{\text{ref}} = \begin{bmatrix} V^{\text{ref}}_{1,1} \\ V^{\text{ref}}_{1,2} \\ V^{\text{ref}}_{2,2} \\ a_3E^{\text{ref}}_{2,3} \\ a_3E^{\text{ref}}_{3,3} \\ V^{\text{ref}}_{3,4} \\ V^{\text{ref}}_{4,5} \\ V^{\text{ref}}_{4,6} \end{bmatrix}, \quad [V]^{\text{inc}} = \begin{bmatrix} V^{\text{inc}}_{1,1} \\ V^{\text{inc}}_{1,2} \\ V^{\text{inc}}_{2,2} \\ a_3E^{\text{inc}}_{2,3} \\ a_3E^{\text{inc}}_{3,3} \\ V^{\text{inc}}_{3,4} \\ V^{\text{inc}}_{4,5} \\ V^{\text{inc}}_{4,6} \end{bmatrix}. \tag{3}$$

The parameter a_3 is a normalized constant to make the equations of the same form involving only the unit of volts. The matrix $O_{i\times j}$ presents an $i\times j$ zero matrix. The variables $\rho_1 = 0$ and $\rho_4 = -1$, while ρ_5 and ρ_6 are the reflection coefficients of the loads. Node J_3 is an ideal junction, so

$$[\rho]_3 = \begin{bmatrix} 0 & 1 \\ 1 & 0 \end{bmatrix}. \tag{4}$$

For node J_2, the scattering parameters can be derived as the following matrix (5).

$$[\rho]_2 = \begin{bmatrix} \dfrac{Y_0 - Y_g - Y_{ap}}{Y_0 + Y_g + Y_{ap}} & \dfrac{2Y_g}{Y_0 + Y_g + Y_{ap}} \\ \dfrac{2Y_0}{Y_0 + Y_g + Y_{ap}} & \dfrac{Y_g - Y_0 - Y_{ap}}{Y_0 + Y_g + Y_{ap}} \end{bmatrix} \tag{5}$$

where Y_0 is the field admittance in free space, $Y_g = 1/Z_{gmn}$ is the field admittance of TE and TM modes in cavity, $Y_{ap} =$

$1/Z_{ap}$, and the aperture impedance Z_{ap} can be expressed as follows [16]:

$$Z_{ap} = \frac{1}{2} jC_m Z_{0s} \tan(k_0 l/2) \tag{6}$$

where k_0 is the propagation constant in free space and C_m is the multimode modal coupling coefficient given by [17]. For multiple apertures on the same wall, the total aperture impedance can be calculated by simply integrating all the individual aperture impedances [18].

B. TUBE PROPAGATION RELATIONSHIP

Ignoring the radiation from the TL in the enclosure, the tube propagation relationship can be written as

$$[V]^{ref}_{8\times1} = [\Gamma]_{8\times8}[V]^{inc}_{8\times1} - [V_s]_{8\times1} \tag{7}$$

where $[V_s] = [V_0\ 0\ 0\ 0\ 0\ 0\ 0\ 0]^T$ and the propagation matrix is expressed as

$$[\Gamma] = \begin{bmatrix} [\Gamma]_1 & O_{2\times2} & O_{2\times2} & O_{2\times2} \\ O_{2\times2} & [\Gamma]_2 & O_{2\times2} & O_{2\times2} \\ O_{2\times2} & O_{2\times2} & [\Gamma]_3 & O_{2\times2} \\ O_{2\times2} & [F]_1 & [F]_2 & [\Gamma]_4 \end{bmatrix} \tag{8}$$

The source voltage V_0 represents the external incident EM field, and

$$[\Gamma]_i = \begin{bmatrix} 0 & e^{\gamma_i l_i} \\ e^{\gamma_i l_i} & 0 \end{bmatrix} \tag{9}$$

where γ_i and l_i are the propagation constant and the length of the i^{th} tube, respectively.

$$[F]_1 = \begin{bmatrix} 0 & -F_1'/a_3 \\ 0 & -F_2'/a_3 \end{bmatrix} \text{ and } [F]_2 = \begin{bmatrix} -F_1''/a_3 & 0 \\ -F_2''/a_3 & 0 \end{bmatrix} \tag{10}$$

are the functions to describe the different modal fields coupling to the TLs at the node J_3. The explicit expressions of those F functions are the key to solve the equations (7) – (9). To achieve this, the distributed voltage source along the TLs is first expressed as (11) based on Agrawal model [19].

$$\begin{aligned} V_s(y_s) &= E_y\left(\frac{a}{2}, y_s, d-h\right) - E_y\left(\frac{a}{2}, y_s, d\right) \\ &= -\sum_m \sum_n E^{inc}_{2,3} A \sin\left(\frac{m\pi}{2}\right) \cos\left(\frac{n\pi y_s}{b}\right) \end{aligned} \tag{11}$$

where the coefficient A is derived as [20]

$$A = \begin{cases} \sqrt{\varepsilon_m \varepsilon_n}\dfrac{m}{a}\left(m^2\dfrac{b}{a} + n^2\dfrac{a}{b}\right)^{-1/2}, & \text{TE modes} \\ \dfrac{2n}{b}\left(m^2\dfrac{b}{a} + n^2\dfrac{a}{b}\right)^{-1/2}, & \text{TM modes} \end{cases} \tag{12}$$

where $m, n = 0, 1, 2, 3\ldots$, and

$$\begin{cases} \varepsilon_m = 1 & \text{if } m = 0 \\ \varepsilon_m = 2 & \text{if } m \neq 0, \end{cases} \quad \begin{cases} \varepsilon_n = 1 & \text{if } n = 0 \\ \varepsilon_n = 2 & \text{if } n \neq 0 \end{cases} \tag{13}$$

Additionally, there are two lumped voltage sources at the terminals of the TLs, which are given in terms of the z-component of the E-field (see Fig. 1 (a)) and can be expressed as

$$\begin{aligned} V_N &= -\int_{d-h}^{d} E_z\left(\frac{a}{2}, y_N, z\right) dz \\ &= -\int_{d-h}^{d} \sum_m \sum_n E^{inc}_{2,3} B \sin\left(\frac{m\pi}{2}\right) \sin\left(\frac{n\pi y_N}{b}\right) dz \end{aligned} \tag{14}$$

where

$$B = -\frac{2\pi}{abk_g} \frac{1}{\tan(k_g(d-z))} \left(m^2\frac{b}{a} + n^2\frac{a}{b}\right)^{1/2} \tag{15}$$

and γ_g is the propagation constant of the traveling wave in the rectangular waveguide. The variable $N = 1, 2$ represents the two terminals of the TL. Only TM modes are taken into consideration because $E_z^{TE} = 0$.

Considering the voltage sources discussed above, the source terms for the modal fields coupling to TLs in the Agrawal model can be written as

$$\begin{bmatrix} S_1' \\ S_2' \end{bmatrix} = \begin{bmatrix} \dfrac{1}{2}\displaystyle\int_{y_1}^{y_2} e^{\gamma_4 y_s} V_s(y_s)\, dy_s - \dfrac{V_1}{2} + \dfrac{V_2}{2} e^{\gamma_4 L} \\ -\dfrac{1}{2}\displaystyle\int_{y_1}^{y_2} e^{\gamma_4 (L-y_s)} V_s(y_s)\, dy_s + \dfrac{V_1}{2} e^{\gamma_4 L} - \dfrac{V_2}{2} \end{bmatrix} \tag{16}$$

Finally, the F functions are derived as

$$\begin{bmatrix} F_1' \\ F_2' \end{bmatrix} = \begin{bmatrix} S_1'/E^{inc}_{2,3} \\ S_2'/E^{inc}_{2,3} \end{bmatrix} \text{ and } \begin{bmatrix} F_1'' \\ F_2'' \end{bmatrix} = \begin{bmatrix} F_1' \\ F_2' \end{bmatrix}. \tag{17}$$

These functions F will change correspondingly when the TL is located along different directions. This is because only those E-field components that are tangential to the TL contribute to the distributed voltage sources and terminal lumped sources.

C. THE EXTENDED BLT EQUATION

By combining (1) and (7), the extended BLT equation is depicted in the summarized form for the model shown in Fig. 1.

$$[V]_{8\times1} = ([I]_{8\times8} + [\rho]_{8\times8})([\Gamma]_{8\times8} - [\rho]_{8\times8})^{-1}[V_s]_{8\times1} \tag{18}$$

where $[V] = [V_{1,1}\ V_{1,2}\ V_{2,2}\ a_3E_{2,3}\ a_3E_{3,3}\ V_{3,4}\ V_{4,5}\ V_{4,6}]^T$ and $[I]$ is an 8×8 unit matrix. Solving this extended BLT equation will provide the voltage response at each node.

III. NUMERICAL VALIDATION AND DISCUSSION

To validate the proposed analytical approach, two configurations as in [10] are studied first. The metallic enclosure is 30 cm × 12 cm × 26 cm. The TL (radius = 0.75 mm, length = 8 cm) parallel to the y-axis is located from $y_1 = 2$ cm to $y_2 = 10$ cm and terminated with a matched impedance $Z_1 = Z_2 = 197\ \Omega$ at each end. Its distance to the back wall, h, is 1 cm. The enclosure is illuminated by a normal

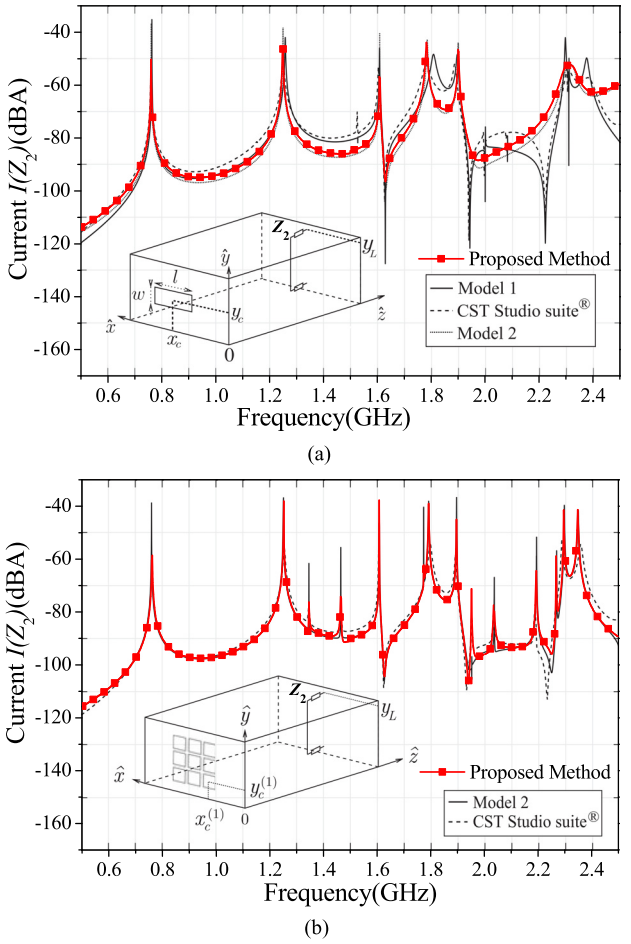

FIGURE 2. Comparison of induced currents at the load Z_2 using different methods, in the cases of (a) a single aperture, and (b) aperture array in [10].

incident EM field in which $E_y = 10$ V/m (see Fig. 1). Here, two different types of apertures are studied: one is a single aperture with size of $l \times w = 6$ cm $\times$ 2 cm, and another is a 3×3 aperture array of 2 cm square holes separated by 0.7 cm in both directions x and y.

The induced currents on the load Z_2 are calculated and compared with the data in [10], which are shown in Fig. 2. For the case of a single aperture, the current values calculated using the proposed analytical functions and the extended BLT equation match well with that simulated by CST, from 0.5 GHz to 2 GHz (Fig. 2a). The mean absolute error is 4.71 dB, which is better than 5.93 dB for model 2 in [10].

For the case of the aperture array, a good agreement is also achieved (Fig. 2b). The mean absolute error of 2.79 dB using the proposed approach is smaller than 2.93 dB for model 2 in [10] over the frequency range of 0.5 GHz to 2.5 GHz. It should be noted that the proposed analytical approach has taken into account the multimode field propagation and bidirectional interaction between the external and the internal fields through the scattering matrix at the aperture coupling node J_2. When the frequency increases above 2 GHz, the accuracy of the proposed method decreases. The reason is that the accuracy of aperture admittance calculation based on

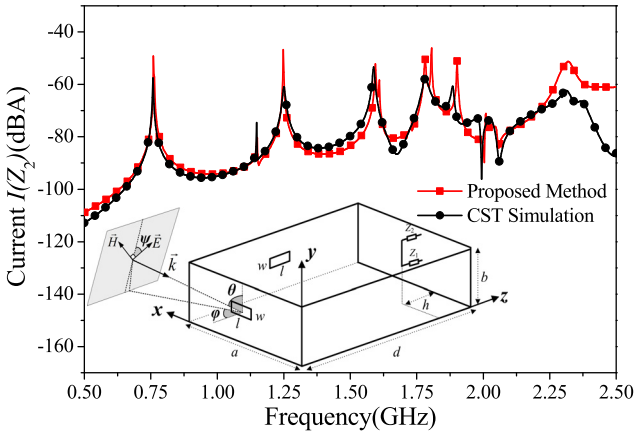

FIGURE 3. The induced current at the load Z_2 of the TL inside an enclosure with apertures on multiple walls and illuminated by oblique incident EM field.

the equivalent circuit method decreases with the increase of frequency, resulting in less accurate modeling of electromagnetic fields in the enclosure, and therefore, the evaluation of the load response deviates more. Another reason might be that the radiation from the TLs may increase at higher frequencies, which is not considered in the proposed model.

To prove the flexible feasibility of the proposed approach, three additional configurations are introduced for further study and validation. The first configuration is the same as in Fig. 2(a) except that the enclosure has apertures on multiple walls and is illuminated by an oblique incident EM field (Fig. 3). Two apertures with dimensions of $l \times w = 6$ cm $\times$ 2 cm are centered on the front wall at $z = 0$ and left wall at $x = a$. The oblique incident EM field with azimuth angle $\varphi = 30°$, elevation angle $\theta = 90°$ and polarization angle $\psi = 0°$ is decomposed into two normal incident components. One is in the $+z$ direction, and the other is in the $-x$ direction. The proposed method can be easily and effectively extended to such an interaction problem by adding another three tubes and four nodes to the original signal flow diagram as shown in Fig. 1(b), leading to 14×14 reflection and propagation matrices and 14×1 voltage and source matrices in (18).

It is shown in Fig. 3 that the induced current derived by the proposed approach matches well with that simulated by CST. The mean absolute error is 3.97 dB over the frequency range of 0.5 GHz to 2.5 GHz. The absolute mean error is 2.78 dB when the frequency is below 2.3 GHz.

Fig. 4 illustrates the second configuration, in which the induced current on load Z_2 of the TL is analyzed. The enclosure (32 cm $\times$ 18 cm $\times$ 12 cm) has an off-centered aperture of 3 cm $\times$ 3 cm, located at point P_1(65 mm, 75 mm, 0 mm). The shortest side of the enclosure is along the z-direction, leading to the dominant resonant mode TM_{110}. The incident EM field and load impedance are the same as that in Fig. 2(a). The TL has the same length and radius as in the previous cases except that the center of the TL is located at point P_2 (100 mm, 50 mm, 110 mm). The calculated results have revealed that the induced current predicted by the analytical approach matches well with that simulated by CST. The mean

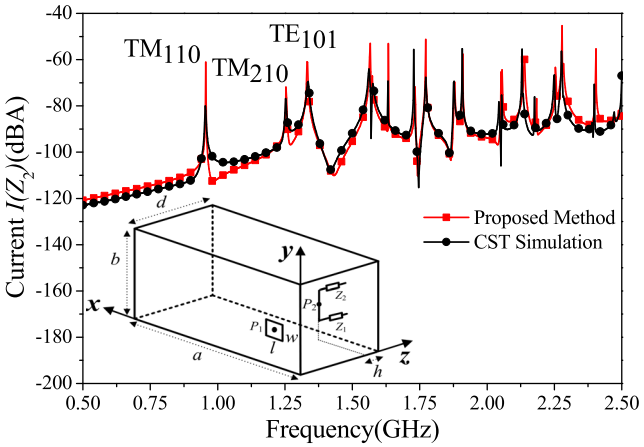

FIGURE 4. The induced current at the load Z_2 of the TL inside an enclosure with an off-centered aperture.

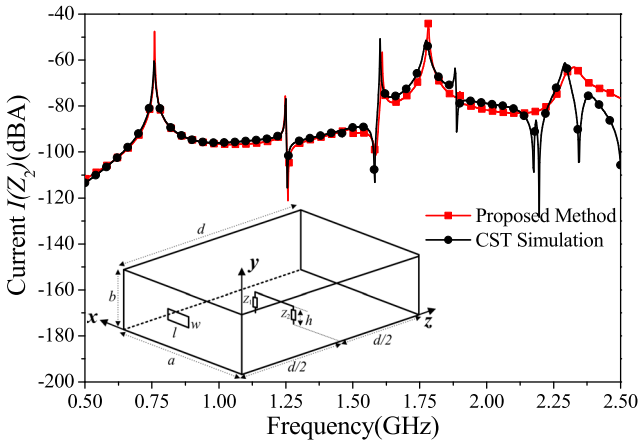

FIGURE 5. The induced current at the load Z_2 of TL in a different direction (parallel to x-axis) inside an enclosure.

absolute error is 3.52 dB, and all the resonant frequencies have been explicitly predicted in Fig. 4.

Fig. 5 shows the induced current on load Z_2 of the TL located in a different direction (parallel to x-axis). The TL is centered on the bottom wall of the enclosure and terminated by matched impedance at both terminals. The distance between the TL and the bottom wall, h, is 1 cm. The same geometric parameters of the TL are used. In this case study, the field components of E_x and E_y are taken into consideration to calculate the source terms in (16). Note that the distributed voltage source along the TL in this case is expressed as

$$V_s(x_s) = E_x\left(x_s, h, \frac{d}{2}\right) - E_x\left(x_s, 0, \frac{d}{2}\right) = \sum_m \sum_n E_{2,3}^{\text{inc}} C \cos\left(\frac{m\pi x_s}{a}\right) \sin\left(\frac{n\pi h}{b}\right) \quad (19)$$

The coefficient C is given as [20]

$$C = \begin{cases} \sqrt{\varepsilon_m \varepsilon_n}\dfrac{n}{b}\left(m^2\dfrac{b}{a} + n^2\dfrac{a}{b}\right)^{-1/2}, & \text{TE modes} \\ \dfrac{2m}{a}\left(m^2\dfrac{b}{a} + n^2\dfrac{a}{b}\right)^{-1/2}, & \text{TM modes} \end{cases} \quad (20)$$

where the values of ε_m and ε_n are the same as in (13).

The results in Fig. 5 illustrate that the current predicted by the proposed method also agree well with those from numerical simulation, with a mean absolute error of 3.24 dB. This again demonstrates the flexibility of the proposed method for different orientations and locations of TLs in an enclosure.

The agreement between the results using the proposed analytical approach and those from numerical simulation validates the efficiency of the proposed analytical expressions of the scattering functions and coupling functions at the specified nodes J_2 and J_3 in extended BLT equation. Moreover, the calculation takes only a dozen seconds using the proposed method, while the numerical simulation needs more than 4 hours.

IV. CONCLUSION

A few efficient analytical algorithms have been proposed to study the external electromagnetic field coupling to TLs in a metallic enclosure. First, the scattering matrix for the extended BLT equation is derived in an analytical form to model the aperture coupling as a junction, instead of numerical modeling. Second, the coupling functions to model the effect of internal modal fields coupling to TLs are deduced based on the topology method. These proposed analytical functions enable the extended BLT equation to directly and effectively analyze external EM field interaction with TLs in metallic enclosures with apertures. It should be noted that the computational efficiency for such electromagnetic interference problems has also been improved greatly by using the proposed analytical approach. For instance, it is reduced by approximately 1200 times compared to CST numerical simulation for the cases studied in the paper. Though the proposed model is derived in the frequency domain, the induced current at the terminated loads of TLs in metallic enclosures exposed to electromagnetic pulses can also be analyzed by solving the problem in the frequency domain first and then converting to transient response via inverse Fourier Transformation. More importantly, the proposed approach can be easily and effectively extended for integrated and complicated system-level problems where a series of similar configurations are used. It would be especially beneficial for smart cities since more and more electromagnetic fields (or noise) impinge upon the modern electrical and electronic systems.

REFERENCES

[1] W. P. Carpes, L. Pichon, and A. Razek, "Analysis of the coupling of an incident wave with a wire inside a cavity using an FEM in frequency and time domains," *IEEE Trans. Electromagn. Compat.*, vol. 44, no. 3, pp. 470–475, Aug. 2002.

[2] Z. Fei, Y. Huang, J. Zhou, and C. Song, "Numerical analysis of a transmission line illuminated by a random plane-wave field using stochastic reduced order models," *IEEE Access*, vol. 5, pp. 8741–8751, May 2017.

[3] T. V. Yioultsis, T. I. Kosmanis, I. T. Rekanos, and T. D. Tsiboukis, "EMC analysis of high-speed on-chip interconnects via a mixed quasi-static finite difference—FEM technique," *IEEE Trans. Magn.*, vol. 43, no. 4, pp. 1365–1368, Apr. 2007.

[4] W. P. Carpes, Jr., G. S. Ferreira, A. Raizer, L. Pichon, and A. Razek, "TLM and FEM methods applied in the analysis of electromagnetic coupling," *IEEE Trans. Magn.*, vol. 36, no. 4, pp. 982–985, Jul. 2000.

[5] H. D. Bruns, C. Schuster, and H. Singer, "Numerical electromagnetic field analysis for EMC problems," *IEEE Trans. Electromagn. Compat.*, vol. 49, no. 2, pp. 253–262, May 2007.
[6] H. Xie, J. Wang, R. Fan, and Y. Liu, "A hybrid FDTD-SPICE method for transmission lines excited by a nonuniform incident wave," *IEEE Trans. Electromagn. Compat.*, vol. 51, no. 3, pp. 811–817, Aug. 2009.
[7] T. Konefal *et al.*, "Electromagnetic coupling between wires inside a rectangular cavity using multiple-mode-analogous-transmission-line circuit theory," *IEEE Trans. Electromagn. Compat.*, vol. 43, no. 3, pp. 273–281, Aug. 2001.
[8] A. Boutar, A. Reineix, C. Guiffaut, and G. Andrieu, "An efficient analytical method for electromagnetic field to transmission line coupling into a rectangular enclosure excited by an internal source," *IEEE Trans. Electromagn. Compat.*, vol. 57, no. 3, pp. 565–573, Jun. 2015.
[9] S. V. Tkatchenko, R. Rambousky, and J. B. Nitsch, "Electromagnetic field coupling to a thin wire located symmetrically inside a rectangular enclosure," *IEEE Trans. Electromagn. Compat.*, vol. 55, no. 2, pp. 334–341, Apr. 2013.
[10] A. Rabat, P. Bonnet, K. El Khamlichi Drissi, and S. Girard, "Analytical models for electromagnetic coupling of an open metallic shield containing a loaded wire," *IEEE Trans. Electromagn. Compat.*, vol. 59, no. 5, pp. 1634–1637, Oct. 2017.
[11] J. P. Parmantier, "Numerical coupling models for complex systems and results," *IEEE Trans. Electromagn. Compat.*, vol. 46, no. 3, pp. 359–367, Aug. 2004.
[12] P. Kirawanich, S. J. Yakura, and N. E. Islam, "Simulating large electrical systems for wideband pulse interactions using the topological modular junction concept," *IEEE Trans. Plasma Sci.*, vol. 36, no. 2, pp. 435–442, Apr. 2008.
[13] F. M. Tesche and C. M. Butler, "On the addition of EM field propagation and coupling effects in the BLT equation," Holcombe Dept. Elect. Comput. Eng., College Eng. Sci., Clemson, SC, USA, Interact. Notes 588, 2003.
[14] P. Xiao, P.-A. Du, D. Ren, and B.-L. Nie, "A hybrid method for calculating the coupling to PCB inside a nested shielding enclosure based on electromagnetic topology," *IEEE Trans. Electromagn. Compat.*, vol. 58, no. 6, pp. 1701–1709, Dec. 2016.
[15] *CST Microwave Studio*. [Online]. Available: http://www.cst.com
[16] M. P. Robinson *et al.*, "Analytical formulation for the shielding effectiveness of enclosures with apertures," *IEEE Trans. Electromagn. Compat.*, vol. 40, no. 3, pp. 240–248, Aug. 1998.
[17] F. A. Po'ad, M. Z. M. Jenu, C. Christopoulos, and D. W. P. Thomas, "Multimode consideration in the analysis of shielding effectiveness of a metallic enclosure with off-centred apertures," in *Proc. IEEE Int. Symp. RF Microw. Conf.*, Sep. 2006, pp. 306–310.
[18] M. C. Yin and P. A. Du, "An improved circuit model for the prediction of the shielding effectiveness and resonances of an enclosure with apertures," *IEEE Trans. Electromagn. Compat.*, vol. 58, no. 2, pp. 448–456, Apr. 2016.
[19] A. K. Agrawal, H. J. Price, and S. H. Gurbaxani, "Transient response of multiconductor transmission lines excited by a nonuniform electromagnetic field," *IEEE Trans. Electromagn. Compat.*, vol. EMC-22, no. 2, pp. 119–129, May 1980.
[20] N. Marcuvitz, *Waveguide Handbook*. Stevenage, U.K.: Peregrinus, 2009, pp. 55–65.

LIPING YAN (M'08–SM'15) was born in Shijiazhuang, China, in 1972. She received the M.S. degree in radio physics and the Ph.D. degree in biomedical engineering from Sichuan University, Chengdu, China, in 1996 and 2003, respectively.

In 1996, she joined the Department of Electronics Engineering, Sichuan University. From 2008 to 2009, she was a Visiting Scholar with the Department of Electrical Engineering and Computer Science, University of Wisconsin-Milwaukee. Since 2009, she has been a Professor with the College of Electronics and Information Engineering, Sichuan University. She has authored/co-authored one book, over 100 papers published in peer-reviewed journals and conferences and led a number of industrial/grant projects. Her research interests include electromagnetic compatibility modeling, electromagnetic field exposure assessment, computational electromagnetics, the design of applicators/probes for biomedical applications, and compact antennas.

XINDAN ZHANG was born in Nanchong, China, in 1993. She received the B.Eng. and M.Eng. degrees in electromagnetic field and microwave technology from Sichuan University, Chengdu, China, in 2015 and 2018, respectively.

Her current research interests include the field coupling to transmission line analysis, the application of electromagnetic topology in electromagnetic compatibility, and computational electromagnetics.

XIANG ZHAO was born in Leshan, China, in 1973. She received the B.S. degree in math, the M.S. degree in radio physics, and the Ph.D. degree in biomedical engineering from Sichuan University, Chengdu, China, in 1994, 1997, and 2005, respectively.

In 1997, she joined the Department of Electronics Engineering. Since 2012, she has been a Professor with the College of Electronics and Information Engineering, Sichuan University. She has published over 90 papers in the peer-reviewed journals and conferences and led a number of grant projects. Her research interests include statistical electromagnetics, electromagnetic compatibility modeling, and electromagnetic environment effects evaluation.

XIAOLAN ZHOU was born in Macheng, China, in 1991. She received the B.Eng. and M.Eng. degrees in electromagnetic field and microwave technology from Sichuan University, Chengdu, China, in 2013 and 2016, respectively.

Since 2016, she has been with Huawei Technologies Co., Ltd., Shenzhen, China, as an EMC Engineer. Her research interests include the electromagnetic compatibility test and modeling.

RICHARD XIAN-KE GAO (S'97–M'01–SM'10) received the B.Eng. and M.Eng. degrees from the Huazhong University of Science and Technology and the Ph.D. degree from the National University of Singapore. He was with different industrial companies, universities, and research institutes over 30 years. He is currently a Senior Scientist and the Group Manager with the National Research Institute of High Performance Computing, Singapore. He also holds visiting professor appointments with the universities. He has published over 70 papers in the referred international journals and conferences and led a lot of industrial/grant projects and new products development. His main research interests include EMC/EMI, antenna, RFID, wireless energy, metamaterials, and robust design and optimization technologies.

Dr. Gao is a Senior Member of Distinguished Lecturer of the IEEE EMC Society. He received various rewards, including the Best Paper Award of APEMC 2016. He is the TPC chairs for APEMC 2020 and APMC 2019. He was the TPC Chair of joint 2018 IEEE EMC and APEMC Symposium. He also served on other executive positions in various international conferences and symposiums. From 2010 to 2011 and from 2016 to 2017, he served as the Chairman of the IEEE Singapore EMC Chapter. He is a Guest Editor of the IEEE Transactions on EMC and serves as a reviewer of prestigious international journals and conferences.